J|A|C|S ARTICLES

Published on Web 04/06/2009

Semisynthetic Fluorescent Sensor Proteins Based on Self-Labeling Protein Tags

Matthias A. Brun, Kui-Thong Tan, Eiji Nakata,† Marlon J. Hinner, and Kai Johnsson*

Institute of Chemical Sciences and Engineering, École Polytechnique Fédérale de Lausanne (EPFL), CH-1015, Lausanne, Switzerland

Received January 8, 2009; E-mail: kai.johnsson@epfl.ch

Abstract: Genetically encoded fluorescent sensor proteins offer the possibility to probe the concentration of key metabolites in living cells. The approaches currently used to generate such fluorescent sensor proteins lack generality, as they require a protein that undergoes a conformational change upon metabolite binding. Here we present an approach that overcomes this limitation. Our biosensors consist of SNAP-tag, a fluorescent protein and a metabolite-binding protein. SNAP-tag is specifically labeled with a synthetic molecule containing a ligand of the metabolite-binding protein and a fluorophore. In the labeled sensor, the metabolite of interest displaces the intramolecular ligand from the binding protein, thereby shifting the sensor protein from a closed to an open conformation. The readout is a concomitant ratiometric change in the fluorescence intensities of the fluorescent protein and the tethered fluorophore. The observed ratiometric changes compare favorably with those achieved in genetically encoded fluorescent sensor proteins. Furthermore, the modular design of our sensors permits the facile generation of ratiometric fluorescent sensors at wavelengths not covered by autofluorescent proteins. These features should allow semisynthetic fluorescent sensor proteins based on SNAP-tag to become important tools for probing previously inaccessible metabolites.

Introduction

The determination of the concentration of metabolites and metal ions with high temporal and spatial resolution in living cells and organisms is an important challenge in biology. For example, progress in neurobiology requires real-time tracking of the secretion and clearance of neurotransmitters, and a detailed understanding of metabolic fluxes requires knowing the concentration of key metabolites in living cells. Fluorescence-based sensors are well suited for measurements in cells and in vivo, as they permit a noninvasive measurement of the analyte of interest. While there are well established strategies to generate fluorescent sensors for specific metal ions based on synthetic fluorophores,[1] the design of sensors for metabolites is still challenging. Most current strategies for sensing metabolites in living cells use Förster resonance energy transfer (FRET) between two autofluorescent proteins (FP).[2] FRET-based sensors are ideal for cellular applications, because they permit a ratiometric measurement of the signal, which makes the sensor response independent of its concentration. Over the last years, a number of FP-based sensors for applications in cells have been developed, such as sensors for amino acids,[3−5] carbohydrates,[6−8] and phosphate.[9] The majority of these sensors rely on a conformational change of a protein upon ligand binding.[2,10−15] Sandwiching such a binding protein between two FPs permits the detection of the ligand through changes in FRET efficiency. Bacterial periplasmic binding proteins are most often used as binding proteins since they undergo the required conformational change upon ligand binding.[16−18]

† Present address: Department of Life System, Institute of Technology and Science, Graduate School, The University of Tokushima, Minami-josanjimacho-2, Tokushima 770-8506, Japan.

(1) Domaille, D. W.; Que, E. L.; Chang, C. J. *Nat. Chem. Biol.* **2008**, *4*, 507.
(2) Wiechert, W.; Schweissgut, O.; Takanaga, H.; Frommer, W. B. *Curr. Opin. Plant Biol.* **2007**, *10*, 323.
(3) Okumoto, S.; Looger, L. L.; Micheva, K. D.; Reimer, R. J.; Smith, S. J.; Frommer, W. B. *Proc. Natl. Acad. Sci. U.S.A.* **2005**, *102*, 8740.
(4) Dulla, C.; Tani, H.; Okumoto, S.; Frommer, W. B.; Reimer, R. J.; Fluguenard, J. R. *J. Neurosci. Methods* **2008**, *168*, 306.
(5) Hires, S. A.; Zhu, Y. L.; Tsien, R. Y. *Proc. Natl. Acad. Sci. U.S.A.* **2008**, *105*, 4411.
(6) Fehr, M.; Frommer, W. B.; Lalonde, S. *Proc. Natl. Acad. Sci. U.S.A.* **2002**, *99*, 9846.
(7) Lager, I.; Looger, L. L.; Hilpert, M.; Lalonde, S.; Frommer, W. B. *J. Biol. Chem.* **2006**, *281*, 30875.
(8) Lager, I.; Fehr, M.; Frommer, W. B.; Lalonde, S. W. *FEBS Lett.* **2003**, *553*, 85.
(9) Gu, H.; Lalonde, S.; Okumoto, S.; Looger, L. L.; Scharff-Poulsen, A. M.; Grossman, A. R.; Kossmann, J.; Jakobsen, I.; Frommer, W. B. *FEBS Lett.* **2006**, *580*, 5885.
(10) Medintz, I. L. *Trends Biotechnol.* **2006**, *24*, 539.
(11) Looger, L. L.; Lalonde, S.; Frommer, W. B. *Plant Physiol.* **2005**, *138*, 555.
(12) Lalonde, S.; Ehrhardt, D. W.; Frommer, W. B. *Curr. Opin. Plant Biol.* **2005**, *8*, 574.
(13) Fehr, M.; Okumoto, S.; Deuschle, K.; Lager, I.; Looger, L. L.; Persson, J.; Kozhukh, L.; Lalonde, S.; Frommer, W. B. *Biochem. Soc. Trans.* **2005**, *33*, 287.
(14) Deuschle, K.; Fehr, M.; Hilpert, M.; Lager, I.; Lalonde, S.; Looger, L. L.; Okumoto, S.; Persson, J.; Schmidt, A.; Frommer, W. B. *Cytometry Part A* **2005**, *64A*, 3.
(15) Fehr, M.; Ehrhardt, D. W.; Lalonde, S.; Frommer, W. B. *Curr. Opin. Plant Biol.* **2004**, *7*, 345.
(16) Shilton, B. H.; Flocco, M. M.; Nilsson, M.; Mowbray, S. L. *J. Mol. Biol.* **1996**, *264*, 350.
(17) Medintz, I. L.; Deschamps, J. R. *Curr. Opin. Biotechnol.* **2006**, *17*, 17.
(18) Dwyer, M. A.; Hellinga, H. W. *Curr. Opin. Struct. Biol.* **2004**, *14*, 495.

The obligatory conformational change in the binding protein severely limits the choice of proteins available for the development of new FRET biosensors.[10] Such proteins must either be identified from natural sources or generated through protein design.[18] Furthermore, since the conformational change of the binding protein is usually small, a careful optimization of each FRET biosensor is frequently necessary to obtain a satisfactory dynamic range (defined as the ratio of the emission ratio of the two fluorescent proteins in the presence of the analyte divided by the emission ratio of the two fluorescent proteins in the absence of the analyte). Such an optimization can be achieved by changing the position of the fluorescent proteins relative to the sensor domain and by varying the length and nature of the linker peptides between the protein units of the biosensor. For example, to improve the dynamic range of a glutamate FRET biosensor from 1.07 to 1.44, the analysis of 176 different mutant sensors with different linker length was necessary.[5] A disadvantage of FPs for the generation of FRET biosensors is that they generally have broad absorption and emission spectra and small Stokes shifts, which often leads to significant cross-talk in both the excitation and emission spectra[19,20] and makes the simultaneous use of more than one biosensor (multiplexing) difficult.[21,22] The necessity for a binding protein that undergoes a conformational change upon ligand binding and the limitations of FPs thus hinders the development of new FRET biosensors for the (simultaneous) sensing of metabolites.

One possibility to increase the choice of fluorophores is a direct chemical labeling of binding proteins with synthetic fluorophores, which is usually achieved via unique cysteine residues.[23] While there are numerous examples for such semisynthetic biosensors,[24,25] their utility for sensing metabolites in living cells is limited because they first need to be assembled in vitro. An alternative approach for the sensing of metabolites employs two surface-tethered components: a binding protein that is labeled with a fluorophore and a ligand that binds to the active site of the binding protein and that is tethered to the surface via a fluorophore-containing linker.[26] The displacement of the ligand from the active site of the binding protein by the analyte of interest leads to a change in FRET. An attractive feature of this system is that it does not rely on a conformational change of the binding protein. However, the approach is not suitable for sensing metabolites in cells or in vivo.

Here we describe a new approach for the generation of fluorescent biosensors based on the SNAP-tag labeling technology. SNAP-tag fusion proteins can be specifically and covalently labeled with O^6-benzylguanine (BG) derivatives in living cells.[27] Our biosensors are comprised of (i) SNAP-tag, (ii) an FP or another self-labeling protein, (iii) a binding protein, and (iv) a synthetic molecule containing a fluorophore and a ligand that can bind to the binding protein (Figure 1). The synthetic molecule is coupled to SNAP-tag via the corresponding BG derivative whereupon the ligand can bind intramolecularly to the binding protein. In the absence of analyte, the biosensor exists in a closed conformation, whereas in the presence of analyte the equilibrium is shifted toward an open conformation. This should lead to a change in the position of the two fluorophores relative to each other and therefore also to a change in the efficiency of FRET between them. As the readout of the system does not depend on a conformational change of the binding protein and since SNAP-tag can be specifically labeled both in vitro and in cells, the approach should permit the generation of an entire family of fluorescent biosensors.

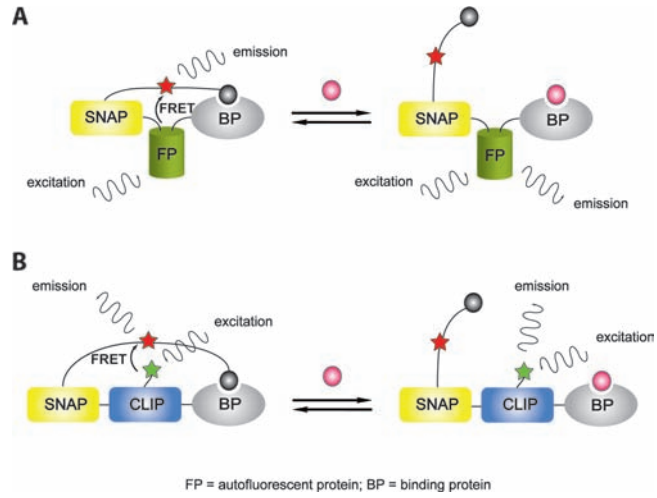

Figure 1. Design principle of the novel semisynthetic sensor proteins. (A) SNAP_FP_BP. The protein part of the sensor is a fusion protein of SNAP-tag, a fluorescent protein, and a binding protein. (B) SNAP_CLIP_BP. The protein part of the sensor is a fusion protein of SNAP-tag, CLIP-tag, and a binding protein. CLIP-tag is used to introduce a synthetic fluorophore (green star). The active semisynthetic sensor for both A and B is obtained by reacting the SNAP-tag of the sensor proteins with a molecule containing a fluorophore (red star) and a ligand for the binding protein (gray ball). In the absence of analyte (pink ball), the intramolecular ligand binds to the binding protein, keeping the biosensor in a closed conformation. According to the design, donor and acceptor fluorophores are in close proximity, resulting in a high FRET efficiency. In the presence of analyte, the intramolecular ligand is displaced, and the biosensor shifts toward an open conformation. Donor and acceptor fluorophore are more distant from each other than in the closed conformation; FRET efficiency therefore decreases.

Results and Discussions

Sensor Design. To prove the applicability of our approach, we chose human carbonic anhydrase II (HCA) as a binding protein. Important for the purpose of our studies, HCA does not undergo a significant conformational change upon ligand binding.[28] It is a ubiquitous enzyme that catalyzes the rapid interconversion of carbon dioxide and hydrogen carbonate. HCA is involved in a variety of biological processes, and inhibitors of the enzyme are highly relevant for clinical applications.[28] The most important class of inhibitors are arylsulfonamides, which bind to the enzyme in a Zn^{2+}-dependent manner. This feature of HCA has been used in several fluorescent indicator systems for the measurement of free Zn^{2+}.[29−31] Our sensor should allow the sensing of both sulfonamides and Zn^{2+} (Figure 2).

(19) Piston, D. W.; Kremers, G. J. *Trends Biochem. Sci.* **2007**, *32*, 407.
(20) Shaner, N. C.; Steinbach, P. A.; Tsien, R. Y. *Nat. Methods* **2005**, *2*, 905.
(21) Ai, H. W.; Hazelwood, K. L.; Davidson, M. W.; Campbell, R. E. *Nat. Methods* **2008**, *5*, 401.
(22) Piljic, A.; Schultz, C. *ACS Chem. Biol.* **2008**, *3*, 156.
(23) De Lorimier, R. M.; Smith, J. J.; Dwyer, M. A.; Looger, L. L.; Sali, K. M.; Paavola, C. D.; Rizk, S. S.; Sadigov, S.; Conrad, D. W.; Loew, L.; Hellinga, H. W. *Protein Sci.* **2002**, *11*, 2655.
(24) Anai, T.; Nakata, E.; Koshi, Y.; Ojida, A.; Hamachi, I. *J. Am. Chem. Soc.* **2007**, *129*, 6232.
(25) Takaoka, Y.; Tsutsumi, H.; Kasagi, N.; Nakata, E.; Hamachi, I. *J. Am. Chem. Soc.* **2006**, *128*, 3273.
(26) Medintz, I. L.; Anderson, G. P.; Lassman, M. E.; Goldman, E. R.; Bettencourt, L. A.; Mauro, J. M. *Anal. Chem.* **2004**, *76*, 5620.
(27) Keppler, A.; Gendreizig, S.; Gronemeyer, T.; Pick, H.; Vogel, H.; Johnsson, K. *Nat. Biotechnol.* **2003**, *21*, 86.
(28) Krishnamurthy, V. M.; Kaufman, G. K.; Urbach, A. R.; Gitlin, I.; Gudiksen, K. L.; Weibel, D. B.; Whitesides, G. M. *Chem. Rev.* **2008**, *108*, 946.

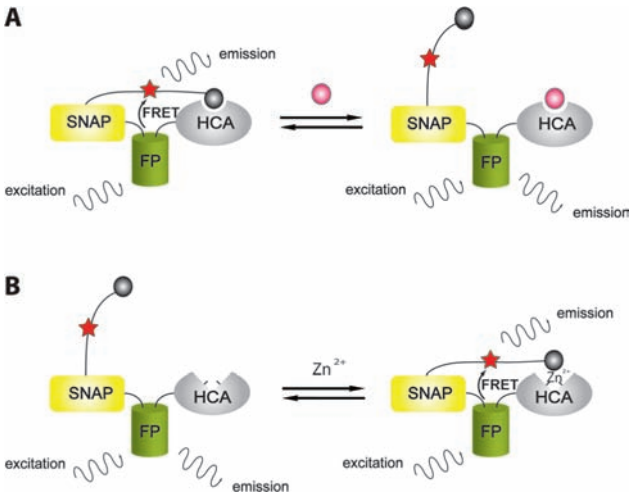

Figure 2. A fluorescent sensor protein for sulfonamides and for Zn^{2+}. (A) SNAP_mCherry_HCA as a biosensor for sulfonamides. In the absence of sulfonamide, the intramolecular ligand binds to HCA; the biosensor is in a closed conformation. In the presence of sulfonamide, the intramolecular ligand is displaced by sulfonamides; the equilibrium is shifted toward an open conformation. This shift should lead to a less efficient FRET between the two fluorophores. (B) SNAP_mCherry_*apo*HCA as a biosensor for Zn^{2+}. The binding of the intramolecular ligand to HCA is Zn^{2+}-dependent. In the absence of Zn^{2+}, the intramolecular ligand does not bind to HCA; the biosensor is in an open conformation. In the presence of Zn^{2+}, the intramolecular ligand binds to the active site of HCA; the equilibrium shifts toward a closed conformation. This shift should lead to a more efficient FRET between the two fluorophores.

Our first sensor protein is a fusion of SNAP-tag, the red FP mCherry,[32] and HCA, yielding SNAP_mCherry_HCA (Figure 2). We designed SNAP_mCherry_HCA to contain a linker of 15 amino acids between SNAP-tag and mCherry and a linker of six amino acids between mCherry and HCA, as well as an N-terminal Strep-tag[33] and a C-terminal 10× His-tag. The fusion protein was expressed in *Escherichia coli* and purified via a two-step affinity purification using Ni-NTA resin followed by Strep-Tactin resin. We obtained pure protein as judged by SDS−PAGE and Coomassie staining (Supporting Information, Figure S1). Analogously, we prepared a second sensor protein, SNAP_CLIP_HCA, in which mCherry was replaced with the self-labeling CLIP-tag.[34] CLIP-tag has orthogonal substrate specificity to SNAP-tag. It reacts with derivatives of O^2-benzylcytosine (CT) and can thus be used to introduce a second synthetic fluorophore and FRET partner into a sensor protein (Figure 1).

Substrates for Labeling. The synthetic precursor for the semisynthetic sensor protein consists of BG, a fluorophore, and the ligand benzenesulfonamide (Chart 1). A derivative of Cy5 was utilized as fluorophore because it is a good FRET acceptor for the donor mCherry (Supporting Information, Figure S2). Alternatively, a derivative of fluorescein was chosen for experiments with SNAP_CLIP_HCA. In both cases, the fluorophore is an integral part of the linker. Benzenesulfonamide was chosen because modifications at the para-position of the benzene ring are known not to perturb its binding affinity to HCA,[35] thereby allowing the attachment of a linker.

The synthesis of the BG derivatives BG-PEG_n-Cy5-SA **1**−**3** with varying polyethylene glycol (PEG) chain lengths and BG-PEG_{11}-fluorescein-SA **5** is described in the Supporting Information. For control experiments we also synthesized BG-PEG_{11}-Cy5 **4** and BG-PEG_{11}-fluorescein **6** lacking the benzenesulfonamide ligand (Chart 1, Supporting Information).

Sulfonamide Sensing. The main experiments were performed with the sensor obtained by labeling SNAP_mCherry_HCA with BG-PEG_{11}-Cy5-SA. As outlined in Figure 2A, this sensor is designed to detect inhibitors of HCA. In the absence of inhibitor, the sensor should be in a closed conformation, and the close proximity of mCherry and Cy5 should lead to a high FRET efficiency between the fluorophores. In the presence of inhibitor, the intramolecular ligand should be displaced, and the sensor should shift toward an open conformation. This transformation should lead to a change of the emission ratio of the two fluorophores, which can be used to measure the concentration of free sulfonamide.

We labeled SNAP_mCherry_HCA with BG-PEG_{11}-Cy5-SA and confirmed the labeling by SDS−PAGE and in-gel fluorescence scanning (Supporting Information, Figure S3). To displace the intramolecular ligand, we utilized two sulfonamide derivatives with different affinities toward HCA. Benzenesulfonamide (SA, K_d of 660 nM)[35] and ethoxzolamide (ethox, K_d of 200 pM)[36] were used as competing inhibitors. SNAP_mCherry_HCA(PEG_{11}-Cy5-SA) was excited at 530 nm, and its emission spectra for different concentrations of both benzenesulfonamide and ethoxzolamide were measured (Figure 3A). We found a concentration-dependent response of the two emission peaks corresponding to mCherry (610 nm) and Cy5 (670 nm) (Figure 3A). Increasing concentrations of sulfonamide led to an increase of fluorescence emission of mCherry and to a decrease of Cy5 fluorescence, indicating a decreased FRET efficiency. This observation is in line with the expected behavior of the biosensor, since the shift from the closed conformation to the open conformation of SNAP_mCherry_HCA(PEG_{11}-Cy5-SA) should increase the distance between donor fluorophore (mCherry) and acceptor fluorophore (Cy5). The ratio of the emissions at 610 nm (mCherry) and at 670 nm (Cy5), $r = F_{610}/F_{670}$, is plotted in Figure 3B as a function of the concentrations of the two sulfonamide inhibitors. The resulting binding isotherms are sigmoidal for both inhibitors, and their ratio $r_{zero} = F_{610,zero}/F_{670,zero}$ in the absence of ligand and their ratio $r_{sat} = F_{610,sat}/F_{670,sat}$ at saturating concentrations of ligand are almost identical. The binding curve is shifted to lower inhibitor concentrations for ethoxzolamide, the stronger inhibitor (see below for detailed analysis). To characterize the total response of the sensor, we use the total ratio change r_{sat}/r_{zero}, which amounts to 2.0 for both inhibitors.

To verify that the ratio change upon sulfonamide titration is indeed due to a specific displacement of the intramolecular ligand from the active site of HCA, we labeled SNAP_mCherry_HCA with BG-PEG_{11}-Cy5. Since this molecule lacks a benzenesulfonamide moiety, it should not specifically interact with HCA. Upon titration with both benzenesulfonamide and

(29) Fierke, C. A.; Thompson, R. B. *Biometals* **2001**, *14*, 205.
(30) Bozym, R. A.; Thompson, R. B.; Stoddard, A. K.; Fierke, C. A. *ACS Chem. Biol.* **2006**, *1*, 103.
(31) Thompson, R. B.; Maliwal, B. P.; Feliccia, V. L.; Fierke, C. A.; McCall, K. *Anal. Chem.* **1998**, *70*, 4717.
(32) Shaner, N. C.; Campbell, R. E.; Steinbach, P. A.; Giepmans, B. N. G.; Palmer, A. E.; Tsien, R. Y. *Nat. Biotechnol.* **2004**, *22*, 1567.
(33) Schmidt, T. G. M.; Skerra, A. *Nat. Protoc.* **2007**, *2*, 1528.
(34) Gautier, A.; Juillerat, A.; Heinis, C.; Correa, I. R.; Kindermann, M.; Beaufils, F.; Johnsson, K. *Chem. Biol.* **2008**, *15*, 128.
(35) Banerjee, A. L.; Swanson, M.; Roy, B. C.; Jia, X.; Haldar, M. K.; Mallik, S.; Srivastava, D. K. *J. Am. Chem. Soc.* **2004**, *126*, 10875.
(36) Krishnamurthy, V. M.; Semetey, V.; Bracher, P. J.; Shen, N.; Whitesides, G. M. *J. Am. Chem. Soc.* **2007**, *129*, 1312.

Chart 1. Substrates for SNAP-tag Fusion Protein Labeling: (A) BG-PEG$_n$-Cy5-SA with $n = 0$, 11, 27 (compounds **1**−**3**)[a] and (B) BG-PEG$_{11}$-fluorescein-SA **5**[b]

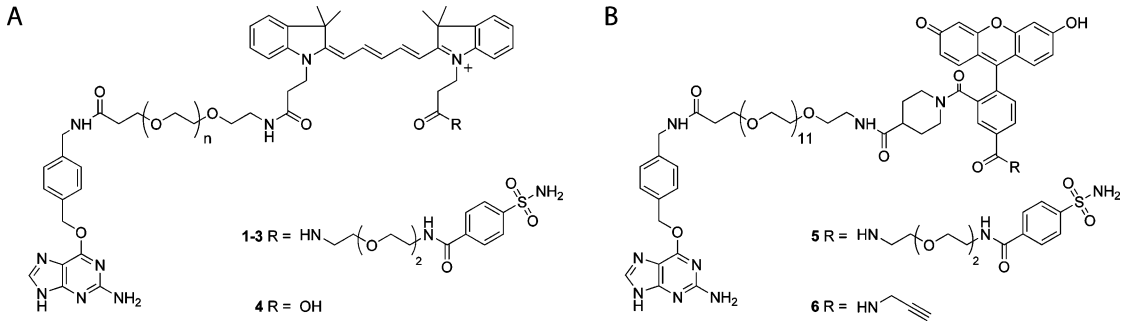

[a] The molecule BG-PEG$_{11}$-Cy5 **4** was used as a control. [b] The corresponding control molecule was BG-PEG$_{11}$-fluorescein **6**.

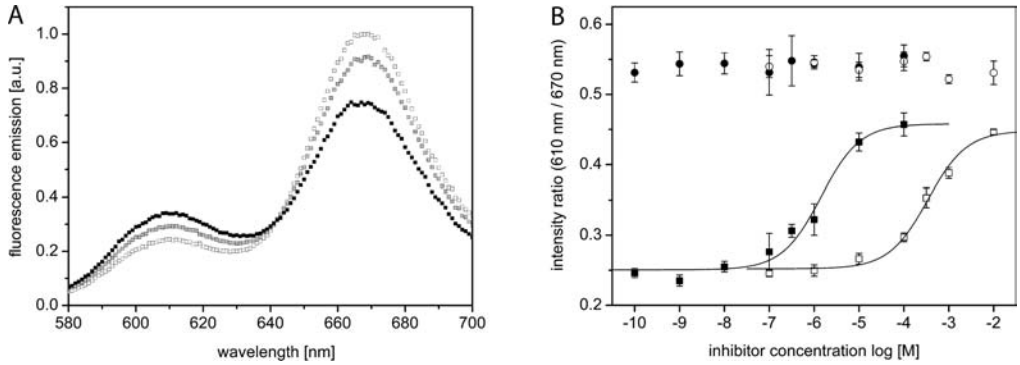

Figure 3. SNAP_mCherry_HCA(PEG$_{11}$-Cy5-SA) as a biosensor for sulfonamides. (A) Emission spectra of SNAP_mCherry_HCA labeled with BG-PEG$_{11}$-Cy5-SA at a low, medium, and high concentration of ethoxzolamide (100 pM, white; 300 nM, gray; 100 μM, black). The addition of ethoxzolamide leads to an increase in the mCherry/Cy5 emission ratio. (B) Fluorescence titration curves. Shown is the ratio of fluorescence of donor (610 nm) and acceptor emission (670 nm) obtained by titrating SNAP_mCherry_HCA(PEG$_{11}$-Cy5-SA) with ethoxzolamide (black squares) and benzenesulfonamide (white squares). SNAP_mCherry_HCA(PEG$_{11}$-Cy5) was used as a control (circles). The data are represented as the mean ± standard deviation of triplicates. The sensor data are fitted according to a single-site binding isotherm.

ethoxzolamide, the fluorescence of SNAP_mCherry_HCA(PEG$_{11}$-Cy5) did not exhibit any dependence on the free inhibitor concentration (Figure 3B). Note that for SNAP_mCherry_HCA(PEG$_{11}$-Cy5-SA) the ratio at saturating concentrations of free ligand is not equal to the ratio of the corresponding sensors labeled with the control molecule BG-PEG$_{11}$-Cy5 (Figure 3B). We attribute this discrepancy to a difference in the chemical structures close to the fluorophore: The negative charge of the carboxylate may affect the electronic properties of the environmentally sensitive fluorophore and therefore its fluorescence. Next, we verified that the covalently linked inhibitor indeed binds intramolecularly and does not induce a noncovalent dimerization of SNAP_mCherry_HCA. SNAP_mCherry_HCA was labeled with BG-PEG$_{11}$-Cy5-SA and analyzed by size-exclusion fast-protein liquid chromatography (SE-FPLC). No dimer formation could be detected under the experimental conditions employed. (Supporting Information, Figure S4).

The binding isotherms reflect a competition between the free inhibitor and the intramolecularly bound inhibitor. The binding curve is characterized by a dissociation constant for the competing ligands ($K_d^{comp,ligand}$),[36] which equals the amount of free ligand that needs to be added to displace the intramolecular ligand in 50% of the sensors. We fitted the data for both inhibitors to a single-site binding isotherm (eq 1, Materials and Methods) and obtained $K_d^{comp,SA} = 340 \pm 60$ μM and $K_d^{comp,ethox} = 550 \pm 110$ nM. Note that in the case of ethoxzolamide, the determined K_d^{comp} is close to the protein concentration of 250 nM. Equation 1 is not strictly valid in this case, and the determined K_d^{comp} is therefore an upper limit to the actual value. Nevertheless, with a difference of around 3 orders of magnitude, the measured $K_d^{comp,ligand}$ values reflect the relative binding affinities of the two inhibitors.

Signal Deconvolution. Environmentally sensitive dyes respond with a change in fluorescence to a change in the polarity of their surroundings. We wanted to investigate to which extent a change of the Cy5 environment upon intramolecular binding might contribute to the response of SNAP_mCherry_HCA(PEG$_{11}$-Cy5-SA). For this purpose, we labeled SNAP_CLIP_HCA with BG-PEG$_{11}$-Cy5-SA as the only fluorophore and measured emission spectra in the absence and presence of free inhibitor (Supporting Information, Figure S5A). We found that Cy5 fluorescence increased in the closed conformation by a non-FRET effect with a factor of $R_{non\text{-}FRET,Cy5} = F_{670,zero}/F_{670,sat} = 1.25 \pm 0.04$ ($n = 4$).

We then investigated whether the total response of the sensor results solely from a combination of FRET and the change of the Cy5 environment or if additional factors need to be considered. The fluorescence ratios due to FRET should be equal for the donor (mCherry at 610 nm) and the acceptor (Cy5 at 670 nm). For three independent measurements, we found an average mCherry fluorescence ratio change and standard deviation of $R_{mCherry}^{FRET} = F_{610,sat}/F_{610,zero} = 1.44 \pm 0.03$. The fluorescence ratio change of Cy5 due to FRET cannot be obtained directly from the measured fluorescence of Cy5 (F_{670}), since F_{670} is the sum of the fluorescence intensities of Cy5 due to (i) FRET, (ii) direct excitation of Cy5, and (iii) mCherry emission at 670 nm,

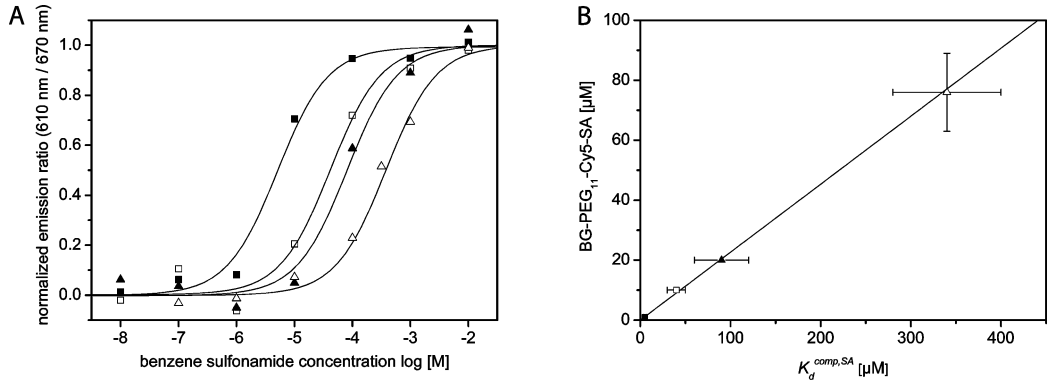

Figure 4. Effective molarity of the intramolecular ligand. (A) Fluorescence titration curves. SNAP_mCherry_HCA quenched with BG and incubated with BG-PEG_{11}-Cy5-SA (1 μM, black squares; 10 μM, white squares; 20 μM, black triangles) was titrated with benzenesulfonamide. The titration curve for SNAP_mCherry_HCA(PEG_{11}-Cy5-SA) is depicted using white triangles for comparison. The fit curves corresponding to a single-site binding isotherm are depicted as solid lines. For clarity, the data (mean of triplicates) are normalized to the respective fitted values of maximum and minimum fluorescence. (B) Determination of the effective molarity of the intramolecular ligand of SNAP_mCherry_HCA(PEG_{11}-Cy5-SA) by linear extrapolation of the $K_d^{comp,SA}$ values obtained from part A. The $K_d^{comp,SA}$ for known concentrations of free BG-$(PEG)_{11}$-Cy5-SA were used to calibrate the local concentration axis assuming a linear relationship (1 μM, black square; 10 μM, white square; 20 μM, black triangle; SNAP_mCherry_HCA(PEG_{11}-Cy5-SA), white triangle).

with $F_{670} = F_{670}^{FRET,Cy5} + F_{670}^{direct,Cy5} + F_{670}^{mCherry}$. In the absence of inhibitor, i.e., in the closed conformation, the environmental non-FRET effect additionally modulates Cy5 fluorescence according to $F_{670,zero} = (F_{670,zero}^{FRET,Cy5} + F_{670,sat}^{direct,Cy5}) \times R_{non\text{-}FRET,Cy5} + F_{670,zero}^{mCherry}$. We obtained $F_{670,sat}^{direct,Cy5}$ and $F_{670,zero}^{mCherry}$ by comparing the spectra depicted in Figure 3A with spectra of unlabeled SNAP_mCherry_HCA and SNAP_CLIP_HCA(PEG_{11}-Cy5-SA) (Supporting Information, Figure S5B). Using these values and $R_{non\text{-}FRET,Cy5} = 1.25$, we calculate $F_{670,sat}^{FRET,Cy5}$ and $F_{670,zero}^{FRET,Cy5}$ from the experimental fluorescence at 670 nm (F_{670}) and obtain $R_{Cy5}^{FRET} = F_{670,zero}^{FRET,Cy5}/F_{670,sat}^{FRET,Cy5} = 1.36$ (cf. Supporting Information, Figure S5B for details). The good agreement with the corresponding value for mCherry $R_{mCherry}^{FRET} = 1.44 \pm 0.03$ indicates that the magnitude of the environmental effect on Cy5 fluorescence in SNAP_mCherry_HCA(PEG_{11}-Cy5-SA) is similar to that observed with SNAP_CLIP_HCA(PEG_{11}-Cy5-SA). The response of SNAP_mCherry_HCA(PEG_{11}-Cy5-SA) is therefore due to an environmental effect and the combined FRET changes of mCherry and Cy5.

Effective Molarity. To further characterize SNAP_mCherry_HCA(PEG_{11}-Cy5-SA), we determined the effective molarity (M_{eff}) of the intramolecularly bound ligand. The effective molarity is defined as the concentration of free ligand that is necessary to displace half of the identical intramolecular ligand. For our sensor, a direct titration of SNAP_mCherry_HCA(PEG_{11}-Cy5-SA) with free BG-PEG_{11}-Cy5-SA is precluded for practical reasons, due to the limited solubility and strong fluorescence of BG-PEG_{11}-Cy5-SA. We therefore determined M_{eff} indirectly, taking advantage of the fact that displacing noncovalently bound BG-PEG_{11}-Cy5-SA by HCA inhibitors also leads to a fluorescence change (Supporting Information, Figure S6). For these experiments, SNAP_mCherry_HCA was quenched with an excess of BG to render a covalent reaction with BG-PEG_{11}-Cy5-SA impossible. The addition of BG-PEG_{11}-Cy5-SA to quenched SNAP_mCherry_HCA leads to an intermolecular interaction of the benzenesulfonamide ligand and HCA. The addition of simple benzenesulfonamide displaces BG-PEG_{11}-Cy5-SA from HCA. Analogously to the displacement of the intramolecular ligand, the competition of free BG-PEG_{11}-Cy5-SA vs benzenesulfonamide can be followed by the ratio change of donor and acceptor fluorophore. By measuring the amount of benzenesulfonamide necessary to displace free BG-PEG_{11}-Cy5-SA at different concentrations of BG-PEG_{11}-Cy5-SA and knowing $K_d^{comp,SA}$, we can obtain the effective molarity of the intramolecular BG-PEG_{11}-Cy5-SA by linear extrapolation. We performed the experiment for three concentrations of BG-PEG_{11}-Cy5-SA and obtained intermolecular $K_d^{comp,SA}$ values of 5.1 ± 1.4, 40 ± 10, and 90 ± 30 μM for the displacement of 1, 10, and 20 μM of free BG-PEG_{11}-Cy5-SA, respectively (Figure 4A). The relative binding affinity of BG-PEG_{11}-Cy5-SA and its parent compound benzenesulfonamide are thus comparable. By extrapolation, we find that the intramolecular $K_d^{comp,SA}$ of SNAP_mCherry_HCA labeled with BG-PEG_{11}-Cy5-SA, 340 ± 60 μM, corresponds to an effective molarity of 80 ± 10 μM for the intramolecular ligand (Figure 4B). We then tested the impact of linker length on the effective molarity by labeling SNAP_mCherry_HCA with BG-Cy5-SA, which possesses no PEG linker, and BG-PEG_{27}-Cy5-SA, a molecule with a linker of 27 PEG units (Supporting Information, Figure S7). The biosensors were titrated with benzenesulfonamide as described above. The fitted values for $K_d^{comp,SA}$ and the corresponding M_{eff} values, obtained by linear extrapolation (Figure 4B), are given in Table 1. Within the experimental error, the linker length had no influence on $K_d^{comp,SA}$ and the derived M_{eff} values.

Table 1. $K_d^{comp,SA}$ Values and Derived M_{eff} Values for SNAP_mCherry_HCA(PEG_n-Cy5-SA), $n = 0, 11, 27$[a]

n	$K_d^{comp,SA}$ (μM)	M_{eff} (μM)
0	350 ± 60	80 ± 10
11	340 ± 60	80 ± 10
27	470 ± 150	110 ± 30

[a] n is the number of PEG units in the linker. The M_{eff} values were estimated using the linear equation M_{eff} (μM) $= 0.22672 \times K_d^{comp,SA}$ (μM).

It is instructive to compare the observed effective molarity of our intramolecular ligand to the one that was recently reported for a similar intramolecular protein−ligand system.[36] In the latter, a benzenesulfonamide derivative was attached covalently to the surface of HCA, close to the active site, with different linker lengths between the attachment site and the inhibitor, yielding effective molarities in the range from 0.8 to 26 mM. The significantly lower M_{eff} value of our system can be explained by the fact that the intramolecular connection between the inhibitor and HCA is much longer, consisting of proteins, flexible peptide linkers, and the PEG linkers in the synthetic part of the sensor. The invariability of the effective molarity in

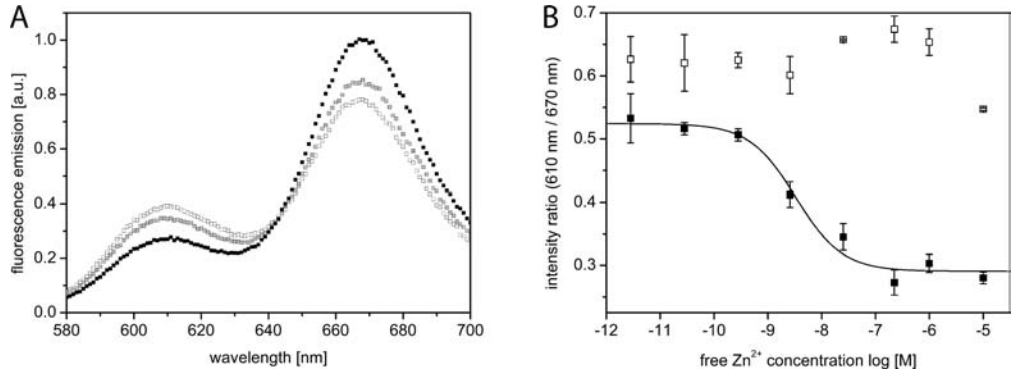

Figure 5. SNAP_mCherry_*apo*HCA(PEG_{11}-Cy5-SA) as a biosensor for Zn^{2+}. (A) Emission spectra of SNAP_mCherry_*apo*HCA labeled with BG-PEG_{11}-Cy5-SA at a low, medium, and high concentration of free Zn^{2+} (1 pM, white; 1 nM, gray; 1 μM, black circles). The addition of free Zn^{2+} leads to a decrease of the mCherry/Cy5 emission ratio. (B) Free Zn^{2+} titration curve for the sensor SNAP_mCherry_*apo*HCA(PEG_{11}-Cy5-SA) (black squares) and control SNAP_mCherry_*apo*HCA(PEG_{11}-Cy5) (white squares). Shown is the ratio of the fluorescence of donor (610 nm) and acceptor emission (670 nm). Data are represented as the mean ± standard deviation of triplicates. The sensor data are fitted according to a single-site binding isotherm.

our system on the synthetic linker length can be rationalized by considering the relatively small change in the total chain length when changing from BG-Cy5-SA via BG-PEG_{11}-Cy5-SA to BG-PEG_{27}-Cy5-SA. Furthermore, the invariability to linker length indicates that there are no steric problems for the covalently attached inhibitor to bind to HCA.

Zn^{2+} Sensing. Having demonstrated the sensing of sulfonamides, we then exploited the fact that the binding of inhibitors to the active site of HCA is Zn^{2+}-dependent. SNAP_mCherry_HCA labeled with BG-PEG_{11}-Cy5-SA should therefore be applicable as a Zn^{2+} sensor: In the absence of Zn^{2+}, the intramolecular ligand should not bind to HCA, and the biosensor should be in an open conformation. In the presence of Zn^{2+}, the intramolecular ligand binds to the active site of HCA. Analogously to the sulfonamide sensing, the shift from the open to the closed conformation of the biosensor should result in a ratio change of mCherry vs Cy5 emission (Figure 2B).

To perform these experiments, we first stripped SNAP_mCherry_HCA of bound Zn^{2+} and then measured the response of the biosensor to added Zn^{2+}. The efficiency of removal of the Zn^{2+} from the active site of HCA was checked using an activity assay with *p*-nitrophenolate acetate as substrate.[25] We found 96% removal of Zn^{2+} from HCA using this procedure (Supporting Information, Figure S8). SNAP_mCherry_*apo*HCA was labeled with BG-PEG_{11}-Cy5-SA (Supporting Information, Figure S9). The assembled sensor was excited at 530 nm, and emission spectra were recorded for different concentrations of free Zn^{2+}. Again, we found concentration-dependent responses of the two emission peaks corresponding to mCherry and Cy5. Increasing concentrations of free Zn^{2+} led to decreased mCherry emission and increased Cy5 emission (Figure 5A). This observation is consistent with the expected behavior of our biosensor, since an increase of free Zn^{2+} should lead to a shift from the open to the closed conformation, leading to increased FRET between mCherry and Cy5. We measured a maximum ratio change of $r_{zero}/r_{sat} = 1.7$ for the response of SNAP_mCherry_*apo*HCA at free Zn^{2+} concentrations below 10 μM. The ratio of the emission at 610 nm (mCherry) and emission at 670 nm (Cy5) $r = F_{610}/F_{670}$ was used to plot the titration curve for free Zn^{2+}. By fitting these data to eq 1, the apparent dissociation constant K_d^{app} for Zn^{2+} was determined to be 2.6 ± 0.6 nM (Figure 5B). This value is in agreement with those reported for a previous Zn^{2+} biosensor based on HCA, which displays apparent dissociation constants in the range of 0.2−0.8 nM.[30] Thus, our sensor protein permits the measurement of free Zn^{2+} at nanomolar concentrations. This concentration range falls well within physiologically relevant free Zn^{2+} concentrations, which range from picomolar to nanomolar in most cell types[37] and up to millimolar in neuronal cells.[37,38]

Control experiments with SNAP_mCherry_*apo*HCA labeled with BG-PEG_{11}-Cy5 did not show any ratio change at concentrations of free Zn^{2+} below 10 μM. This shows that the observed ratio change at free Zn^{2+} concentrations below 10 μM is due to a specific Zn^{2+}-dependent interaction between HCA and the covalently attached benzenesulfonamide. Artificially high Zn^{2+} concentrations above 10 μM caused a further decrease of the 610 nm/670 nm emission ratio of SNAP_mCherry_HCA(PEG_{11}-Cy5-SA) (Supporting Information, Figure S10). Since the biosensor labeled with control molecule **4** exhibits the same phenomenon, the observed effect cannot be due to a specific interaction between the intramolecular ligand and HCA. We assigned the effect to the previously described tendency of multihistidine tag fusion proteins to dimerize at very high concentrations of Zn^{2+}.[39] The potential use of SNAP_mCherry_*apo*HCA as biosensor for Zn^{2+} in living cells would not be affected by this effect, because it could be expressed without a multihistidine tag.

SNAP_CLIP_HCA as Sensor Protein. To demonstrate the versatility of the biosensor concept, we labeled SNAP_CLIP_HCA with different fluorophore pairs. Incubation of SNAP_CLIP_HCA with BG and CT derivatives, substrates for the labeling of SNAP-tag and CLIP-tag, respectively, results in the specific labeling of SNAP_CLIP_HCA. BG-PEG_{11}-Cy5-SA was used in combination with either CT-547 or CT-fluorescein, which are substrates for labeling CLIP-tag with the fluorescent dyes DY-547 and fluorescein, respectively (Supporting Information, Chart S1). We also labeled SNAP_CLIP_HCA with BG-PEG_{11}-fluorescein-SA (Chart 1) and either CT-547 or CT-360, the latter being a substrate for labeling CLIP-tag with the fluorescent dye aminomethylcoumarin (Supporting Information, Chart S1).

The four differently labeled combinations of SNAP_CLIP_HCA were analyzed by SDS−PAGE and in-gel fluorescence scanning (Supporting Information, Figures S11 and S12).

(37) Thompson, R. B. *Curr. Opin. Chem. Biol.* **2005**, *9*, 526.
(38) Kikuchi, K.; Komatsu, K.; Nagano, T. *Curr. Opin. Chem. Biol.* **2004**, *8*, 182.
(39) Evers, T. H.; Appelhof, M. A. M.; Meijer, E. W.; Merkx, M. *Protein Eng. Des. Sel.* **2008**, *21*, 529.

Table 2. Different Fluorophore Pairs for SNAP-tag Based Biosensors

	SNAP-tag	CLIP-tag/FP	maximum ratio change	$K_d^{comp,ligand}$
SNAP_mCherry_HCA	Cy5-SA (**2**)	mCherry	2.0	$340 \pm 60\ \mu M^a$
SNAP_CLIP_HCA	Cy5-SA (**2**)	fluorescein	1.7	290 ± 20 nM^b
SNAP_CLIP_HCA	Cy5-SA (**2**)	DY-547	1.8	340 ± 60 nM^b
SNAP_CLIP_HCA	fluorescein-SA (**5**)	aminomethylcoumarin	1.5	230 ± 40 nM^b
SNAP_CLIP_HCA	fluorescein-SA (**5**)	DY-547	1.3	$220 \pm 70\ \mu M^a$

[a] Benzenesulfonamide was used for the displacement of the intramolecular ligand. [b] Ethoxzolamide was used for the displacement of the intramolecular ligand.

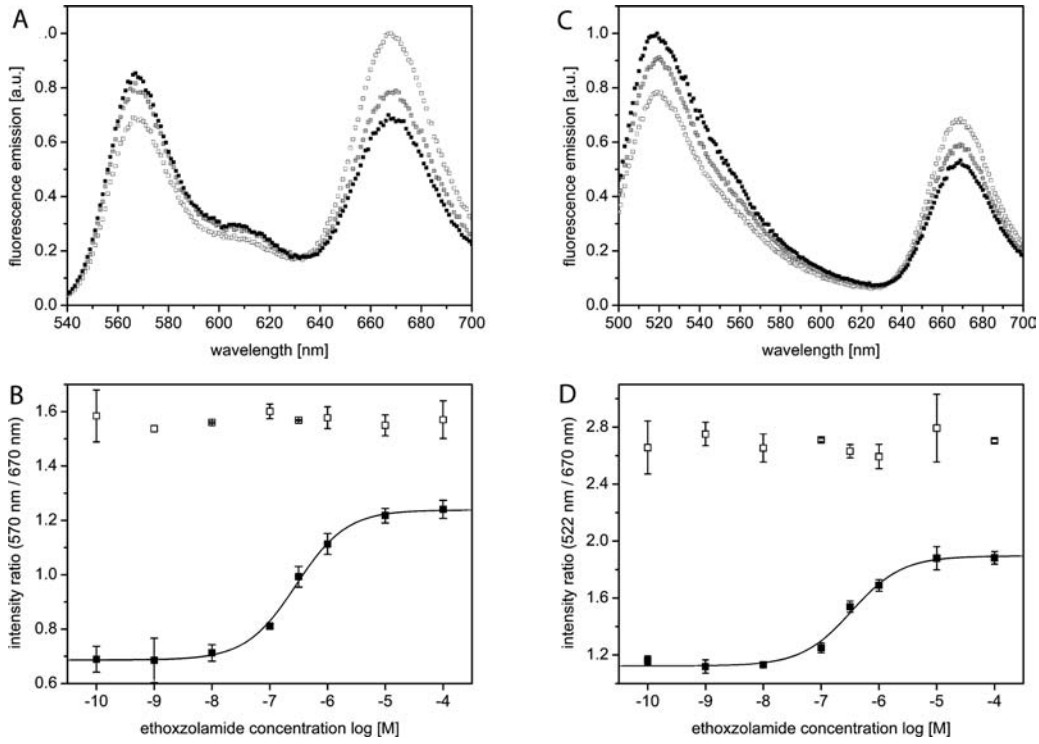

Figure 6. SNAP_CLIP_HCA as a biosensor for sulfonamides. (A) Emission spectra of SNAP_CLIP_HCA labeled with BG-PEG_{11}-Cy5-SA and CT-547 at a low, medium, and high concentration of ethoxzolamide (100 pM, white; 300 nM, gray; 100 μM, black). The addition of ethoxzolamide leads to an increase in the DY547/Cy5 emission ratio. (B) Ethoxzolamide titration curves for SNAP_CLIP_HCA (labeled with BG-PEG_{11}-Cy5-SA and CT-547, black; labeled with the control molecule BG-PEG_{11}-Cy5 and CT-547, white). Data are represented as the mean $\pm$ standard deviation of triplicates. (C) Emission spectra of SNAP_CLIP_HCA labeled with BG-PEG_{11}-Cy5-SA and CT-fluorescein at a low, medium, and high concentration of ethoxzolamide (100 pM, white; 300 nM, gray; 100 μM, black). The addition of ethoxzolamide leads to an increase in the fluorescein/Cy5 emission ratio. (D) Ethoxzolamide titration curves for SNAP_CLIP_HCA (labeled with BG-PEG_{11}-Cy5-SA and CT-fluorescein, black; labeled with the control molecule BG-PEG_{11}-Cy5 and CT-fluorescein, white). Data are represented as the mean $\pm$ standard deviation of triplicates.

Ethoxzolamide or benzenesulfonamide were used to displace the intramolecular ligand from the active site of HCA. All combinations of SNAP_CLIP_HCA labeled with BG-PEG_{11}-fluorophore-SA exhibited a sulfonamide-dependent change of the donor/acceptor emission ratio. Control experiments with BG-PEG_{11}-fluorophore showed no donor/acceptor emission ratio change and proved that the observed response of the biosensor was due to a specific interaction between HCA and the benzenesulfonamide moiety on the BG label [Table 2, Figures 6 and S13 (Supporting Information)]. We obtained very similar maximum ratio changes for the two combinations using BG-PEG_{11}-Cy5-SA as compared to SNAP_mCherry_HCA(PEG_{11}-Cy5-SA), while the maximum ratio changes for the combinations with BG-PEG_{11}-fluorescein-SA were slightly lower (Table 2). This might be due to a larger overlap of the emission spectra of the utilized fluorophore pairs.

Toward Multiplexing. The flexibility with respect to the employed fluorophores should make our semisynthetic protein sensors well-suited for the simultaneous detection of multiple analytes. To explore this idea we labeled SNAP_CLIP_HCA separately with the two different fluorophore pairs fluorescein/aminomethylcoumarin and Cy5/DY-547, using the substrates BG-PEG_{11}-fluorescein-SA/CT-360 and BG-PEG_{11}-Cy5-SA/CT-547, respectively. We combined the two separately labeled sensor proteins and simultaneously measured the response of each to benzenesulfonamide. To ensure spectral orthogonality, the excitation wavelength for the Cy5/DY-547 sensor was increased to 540 nm. From the simultaneously measured benzenesulfonamide-associated ratio changes (Figure 7), we obtained $K_d^{comp,SA}$ values for the fluorescein/aminomethylcoumarin sensor and the Cy5/DY-547 sensor of 220 ± 70 and 270 ± 90 μM, respectively. The simultaneous determination of almost identical $K_d^{comp,SA}$ values for both sensors demonstrate that our semisynthetic sensor proteins are well-suited for the construction of orthogonal FRET pairs. Furthermore, the measured maximum donor/acceptor ratio change and $K_d^{comp,SA}$ of the fluorescein/aminomethylcoumarin sensor were identical to those measured in the absence of the second biosensor (Table

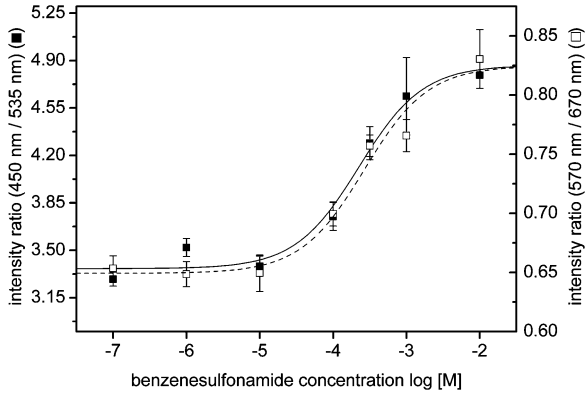

Figure 7. Multiplexing. Benzenesulfonamide titration curves and single-site binding isotherm fit curves for SNAP_CLIP_HCA labeled with BG-PEG_{11}-fluorescein-SA and CT-360 (black squares, solid line) and for SNAP_CLIP_HCA labeled with BG-PEG_{11}-Cy5-SA and CT-547 (white squares, dotted line). Data are represented as the mean ± standard deviation of triplicates.

2). For the pair Cy5/DY-547, the $K_d^{comp,SA}$ was also identical to that measured in the absence of the second biosensor, but the maximum ratio change dropped to 1.3 (Table 2). In conclusion, this proof-of-principle experiment demonstrates how our sensor concept should facilitate the interrogation of multiple biological processes in a simultaneous fashion.

Model of the Sensor. To obtain a qualitative understanding of the molecular mechanism of sensing by SNAP_mCherry_HCA, we took advantage of the utility of FRET efficiency E as a "molecular ruler". The efficiency of FRET is directly connected to the distance d between a fluorescence donor and acceptor by the relation $E = R_0^6/(R_0^6 + d^6)$.[40] The Förster distance R_0 is characteristic for a given fluorescence donor and acceptor pair and can be calculated from their spectral data. For the pair mCherry and Cy5, this calculation yields $R_0^{mCherry/Cy5} = 63$ Å (Materials and Methods, Supporting Information, Figure S1). To obtain E, the fluorescence of the donor mCherry in the absence of a FRET acceptor (F_D) and in the presence of acceptor (F_{DA}) needs to be determined.[40] The FRET efficiency is given by the relation $E = 1 - F_{DA}/F_D$, provided that the labeling of the sensor protein with BG-PEG_{11}-Cy5-SA is complete.[40] We checked the relative absorption of mCherry and Cy5 in the labeled sensor (Materials and Methods) and found it to be consistent with quantitative labeling, which is in accordance with previous reports on SNAP-tag labeling.[41,42]

We determined F_D and F_{DA} in three independent measurements. The corresponding FRET efficiencies in the absence and presence of free inhibitor were $E_{zero} = 0.63 \pm 0.02$ and $E_{sat} = 0.47 \pm 0.03$. Ignoring possible changes in the relative orientation of the transition dipole moments of donor emission and acceptor absorption, we can calculate average apparent distances of $d_{zero} = 57.7$ Å and $d_{sat} = 64.5$ Å. Upon opening of the intramolecular bridge, the apparent distance between Cy5 and mCherry therefore increases by only around 7 Å.

To analyze this result, we constructed a simple model. Figure 8A is a sketch of SNAP_mCherry_HCA(PEG$_{11}$-Cy5-SA) depicting the relevant distances in the protein. The image is drawn to scale and the orientation of the three domains to each other is arbitrary. The distances were estimated as described in the figure caption, using distances taken from crystal structures and a freely jointed chain model for the PEG and peptide linkers. The linkers are described as flexible polymers, and the given distance is the most abundant distance of a broad distance distribution. For the peptide linkers, we assume that our linkers can be approximated by parameters obtained for the linkers described by Merkx.[43] Figure 8B shows the sensor in a conformation in which the sulfonamide binds intramolecularly to HCA (closed conformation). The depicted conformation was chosen to satisfy both the estimated distances within the protein (i.e., the most abundant length of the linkers) and the experimentally determined effective distance between the chromophores (depicted as the section of a red circle in Figure 8B). Our qualitative model together with the experimental data thus suggests that in SNAP_mCherry_HCA, mCherry does not aggregate with either SNAP-tag or HCA. An intramolecular aggregation of SNAP-tag and HCA is also unlikely, as corroborated by the low effective molarities determined experimentally and the negligible impact of linker length on the effective molarities. The observed change in FRET efficiency should thus be due solely to a change in the distance between mCherry and Cy5, with no contribution of changes in the relative orientation of the chromophore dipole moments, as the high flexibility of the linkers should lead to an effective randomization of the relative orientations of mCherry and Cy5. Regarding the change in distance, it should be noted that the flexibility of the linker chains should lead to a broad distribution of distances in the closed and in the open state, with the experimental apparent distances being the effective averages of these distributions.

The absence of intramolecular aggregation should facilitate the future improvement of this sensor. In the open state, the distance between the chromophores is governed by the effective length of the linker between SNAP-tag and mCherry. In the closed state, the distance depends on the linker between mCherry and HCA, provided that it is shorter than the linker between SNAP-tag and mCherry. It should thus be possible to optimize the response of the sensor through linker engineering, i.e., shortening the linker between mCherry and HCA and/or increasing the effective length of the linker between SNAP-tag and mCherry.

Conclusions

We have demonstrated a new approach for the generation of fluorescent biosensor proteins using the SNAP-tag technology. Our novel FRET biosensors are semisynthetic: The genetically encoded part consists of SNAP-tag, a fluorescent protein or CLIP-tag, and a binding protein. The synthetic part is covalently linked to SNAP-tag and contains a fluorophore and a ligand that can bind intramolecularly to the binding protein. In our proof-of-principle sensor, we utilized HCA as the binding protein and benzenesulfonamide as the ligand. The sensors based on the proteins SNAP_mCherry_HCA and SNAP_CLIP_HCA were sensitive to sulfonamides and Zn^{2+}, with a dynamic ratio of up to 2. Thus, the biosensor design can be used to sense analytes that compete with the intramolecular ligand for binding to the active site (sulfonamides) as well as to sense cofactors

(40) Lakowicz, J. R. *Principles of Fluoroscence Spectroscopy*, 3rd ed.; Springer: New York, 2006..
(41) Chidley, C.; Mosiewicz, K.; Johnsson, K. *Bioconjugate Chem.* **2008**, *19*, 1753.
(42) Maurel, D.; Comps-Agrar, L.; Brock, C.; Rives, M. L.; Bourrier, E.; Ayoub, M. A.; Bazin, H.; Tinel, N.; Durroux, T.; Prezeau, L.; Trinquet, E.; Pin, J. P. *Nat. Methods* **2008**, *5*, 561.
(43) Evers, T. H.; van Dongen, E. M. W. M.; Faesen, A. C.; Meijer, E. W.; Merkx, M. *Biochemistry* **2006**, *45*, 13183.

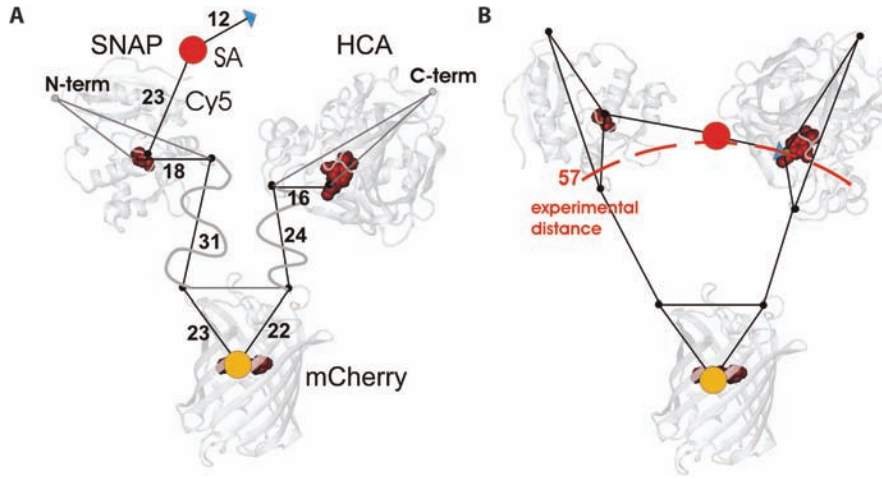

Figure 8. Model of SNAP_mCherry_HCA labeled with BG-PEG$_{11}$-Cy5-SA. (A) Model of the sensor in the open conformation depicting the relevant relative distances in the fusion protein in angstroms. Highlighted are mCherry (orange), Cy5 (red circle), the intramolecular inhibitor benzenesulfonamide (SA, blue triangle), and residues in the active site of each protein (dark red). Distances were estimated as described below. The relative orientation of the three domains to each other is arbitrary. (B) Example for a conformation of the sensor in the closed state. The experimental distance determined from the FRET efficiency and the relation $E = R_0^6/(R_0^6 + d^6)$ is depicted as the dashed section of a circle. Distance calculation: Distances within the proteins were computed from the coordinates in the crystal structures. The C_α of the respective first and last residue resolved in the crystal structure was taken as the N- and C-terminus, respectively. We used a suitable atom in the bound ligand or in the mCherry chromophore for determination of distances to the "active site". Residues that were not resolved in the crystal structure were counted as part of the proteinaceous linkers, leading to linker lengths of 29 amino acids (SNAP-tag/mCherry) and 17 amino acids (mCherry/HCA). The effective length of the proteinaceous linkers was taken as the root-mean-squared distance between the ends of the linkers $\langle r_e^2\rangle^{1/2}$, estimated using a freely jointed chain model with $\langle r_e^2\rangle^{1/2} = (C_n)^{1/2}b_0(n)^{1/2}$,[43] where n is the number of residues in the linkers, b_0 is the average distance between adjacent C_α atoms (3.8 Å), and the characteristic ratio $C_n = 2.3$.[43] The length of the PEG linkers was estimated using the same model, with $(C_n)^{1/2}b_0 = 5.8$ Å.[36] The non-PEG parts of the linker were transformed into equivalent PEG units for the estimation. The length of the linker from SNAP-tag to Cy5 was taken as the equivalent of 16 PEG units and the length of the linker from Cy5 to the inhibitor as four PEG units. The pdb accession codes of the crystal structures are as follows (the atom used to represent the active site is given in parentheses): SNAP-tag, 1EH7 (CS of ligand SMC); mCherry, 2H5Q (CB2 of chromophore CH6); HCA, 2NNG (C7 of ligand CYX).

that are required for the binding of the intramolecular ligand (Zn^{2+}). In both cases, the ratiometric fluorescent response of the sensor is due to a shift from the closed state, where the intramolecular ligand is bound to HCA, to an open state, where the intramolecular ligand is free. We investigated the origin of the signal for SNAP_mCherry_HCA(PEG$_{11}$-Cy5-SA) and found two contributing effects: First, there is a change in FRET efficiency between the two fluorophores in the sensor, because the transition from the closed to the open state leads to a change in their average effective distance. Second, there is a change in fluorescence of Cy5 due to its sensitivity to the different environments in the open and closed state.

In contrast to currently used biosensors, our method does not require a conformational change of the binding protein upon ligand binding. Therefore, every enzyme or binding protein that is known to bind an inhibitor should permit the construction of a biosensor, provided that the linker attachment to the inhibitor does not disrupt its affinity for the binding protein. A further advantage of our method is that a variety of synthetic fluorophores can be employed to construct biosensors. Synthetic fluorophores provide spectroscopic properties, such as increased photostability or red-shifted excitation and emission maxima, which cannot be found in any of the currently existing FPs.[44,45] Notably, the use of fluorophores in the far-red part of the spectrum could provide an increased detectability over background fluorescence in biological samples.[40] Further, the availability of synthetic fluorophores that span the whole visible spectrum facilitates the design of multiple FRET pairs with nonoverlapping spectra. This permits the simultaneous use of orthogonal FRET biosensors in the same sample, i.e. multiplexing.

The concentration range in which SNAP-tag-based sensor proteins can be used to measure a given analyte of interest is determined by the effective molarity of the intramolecular ligand and the binding affinity of the intramolecular ligand relative to the analyte of interest. The effective molarity for SNAP_mCherry_HCA was measured to be around 100 μM and should be similar for sensors based on the same design principle. If the intramolecular ligand and the analyte of interest have an equal binding affinity toward the binding protein, the biosensor can therefore be used to sense the analyte in the 100 μM range. If the analyte has a higher affinity than the intramolecular ligand, the detection range of the sensor is shifted toward lower concentrations; if the analyte has a lower affinity than the intramolecular ligand, the detection range of the sensor is shifted toward higher concentrations. Thus, our method allows tuning the sensitive range of the sensor to the desired concentration by choosing an appropriate intramolecular ligand (if available).

The dynamic range of the presented sensors lies in the upper range that is exhibited by genetically encoded sensors based on periplasmic binding proteins.[10] A further improvement of the dynamic range should be possible by optimization of the linker lengths and flexibilities, because our experimental data have shown that the change in effective distance between the chromophores in the open and closed state is relatively small. Environmentally sensitive dyes could be used to enhance the signal output of the system or for the construction of sensors that rely on this effect alone. For some cellular applications, environmental sensitivity might be a disadvantage, however. In these cases, an environmentally insensitive dye should be

(44) Keppler, A.; Arrivoli, C.; Sironi, L.; Ellenberg, J. *Biotechniques* **2006**, *41*, 167.
(45) Lavis, L. D.; Raines, R. T. *ACS Chem. Biol.* **2008**, *3*, 142.

chosen for sensor construction. Alternatively, the approach is not limited to the use of FRET as the signal output but could also be based on fluorescence polarization.

Although all experiments in this work were done in vitro, we envision future applications of our sensor concept to be on the surface or inside of living cells. The implementation of SNAP-tag based sensor proteins on the cell surface should be a viable approach, since it has been shown that SNAP-tag fusion proteins can be quantitatively labeled on the cell surface of COS-7 cells.[42] Further, the use of membrane-impermeable fluorophores, such as Cy5 derivatives, is especially advantageous in this case, as sensor proteins retained in the secretory pathway are not labeled[42,46] and therefore do not contribute to the background signal. The application of our semisynthetic sensor proteins inside living cells will require cell permeable BG derivatives for efficient SNAP-tag labeling and is probably less straightforward.

In summary, semisynthetic fluorescent sensor proteins based on SNAP-tag are a new class of ratiometric fluorescent sensors that combine high sensitivity with specificity. Their modular design permits the facile generation of ratiometric fluorescent sensors at wavelengths not covered by autofluorescent proteins. Most important, the approach works independently of a conformational change of the protein used for analyte detection. Therefore, the herein presented work provides the basis for the generation of sensor proteins for the detection of previously inaccessible metabolites.

Materials and Methods

Synthesis. Detailed synthetic procedures and characterizations for all synthetic precursors are described in the Supporting Information.

Sensor Construction and Expression. SNAP_mCherry_HCA is composed of SNAP-tag, mCherry, and human carbonic anhydrase II (HCA). SNAP_CLIP_HCA is composed of SNAP-tag, CLIP-tag, and HCA. As the basis for these constructs, we designed a fusion of SNAP-tag and CLIP-tag connected by the linker GR-LEVLFQGPKAFLE. To optimize expression levels, the sequences of SNAP-tag and CLIP-tag were adapted for *E. coli* codon usage with the help of Gene Designer software (DNA2.0, Menlo Park, CA), with codon optimization being done in a manner that minimizes the similarity of both sequences. The genes encoding the constructs SNAP_GRLEVLFQGPKAFLE and GRLEVLFQG-PKAFLE_CLIP were made by Gene Synthesis (Eurofins Medigenomix GmbH, Martinsried, Germany), assembled by PCR, and cloned into the vector pET-51b(+) (Novagen) to obtain pET-51b_SNAP_CLIP. *In-frame* cloning into pET-51b leads to tagging of the insert with an N-terminal Strep-tag II[33] and a C-terminal 10× His-tag. These tags are therefore contained in all constructs based on pET-51b_SNAP_CLIP.

The coding sequence of mCherry was amplified by PCR from the pmCherry-N1 vector (Clontech Laboratories, Inc.) by using the primers mb1 and mb2 (Supporting Information). The PCR fragment was ligated into pET-51b_SNAP_CLIP to replace the coding sequence of CLIP-tag. The resulting construct was named pET-51b_SNAP_mCherry. The coding sequence of HCA was amplified by PCR from a yeast two hybrid human adult colon cDNA library (Dualsystems Biotech) encoding the mature protein using primers mb3 and mb4 (Supporting Information) and inserted into pET51b_SNAP_CLIP and pET-51b_SNAP_mCherry. The resulting plasmids were named pET-51b_SNAP_CLIP_HCA and pET-51b_SNAP-_mCherry_HCA. Protein sequences of both fusion proteins are reported in the Supporting Information.

To express the fusion proteins, the constructs were electroporated into the *E. coli* strain Rosetta-gami (DE3). Bacterial cultures in SB medium were grown at 37 °C to an OD_{600nm} of 0.8. Expression of the fusion proteins was then induced by the addition of 0.5 mM isopropyl β-D-thiogalactopyranoside (IPTG). The bacteria were grown for an additional 16 h at 16 °C and harvested by centrifugation. Cells were lysed by sonication and insoluble protein and cell debris were removed by centrifugation. We used a two-step purification procedure starting with Ni-NTA (Qiagen) followed by *Strep*-Tactin superflow (IBA) according to the instructions of the suppliers. The purified fusion proteins were stored in 50 mM HEPES pH 7.2, 50 mM NaCl at 4 °C until further use. The fusion proteins were stable for several weeks when stored under these conditions. The protein concentration was determined using a Bradford assay with BSA as a standard. Typical protein yields were 0.8−1.2 mg/L of culture medium.

For sensing sulfonamides, the fusion proteins were saturated with $ZnCl_2$ after affinity tag purifications. For sensing Zn^{2+}, the fusion proteins were stripped of Zn^{2+} by dialysis against 50 mM HEPES pH 6.2, 50 mM NaCl, 75 mM dipicolinic acid (DPA) using a Slide-A-Lyzer dialysis cassette (Thermo Scientific) at 4 °C.[47] A second dialysis against 50 mM HEPES, pH 7.2, 50 mM NaCl at 4 °C was performed to subsequently remove DPA.

Biosensor Labeling. The synthesized BG derivatives **1**−**6** and the commercial CT derivatives (Covalys Biosciences, Witterswil, Switzerland) for labeling SNAP-tag and CLIP-tag, respectively, were added to a final concentration of 10 μM to a solution of 5 μM SNAP-tag fusion protein in 50 mM HEPES pH 7.2, 50 mM NaCl, 1 mM dithiothreitol (DTT). The solutions were incubated for 1 h at room temperature. The labeled SNAP-tag fusion proteins were purified from excess BG and CT derivatives using a centrifugal filter device (Microcon YM-50, Millipore). Three washing cycles using 50 mM HEPES pH 7.2, 50 mM NaCl were performed to further purify the derivatized fusion proteins. The labeled fusion proteins were stored at 4 °C until further use.

Size-Exclusion FPLC. 100 μg of the indicated HCA fusion protein was injected onto a Superdex 200 10/300 GL column (GE Healthcare Bio-Sciences, Piscataway, NJ). The column was run in 50 mM HEPES pH 7.2, 50 mM NaCl with a flow rate of 0.4 mL min^{-1}. Protein was detected at 280 nm. The covalent dimer $(SNAP\_mCherry\_HCA)_2$ was used as a control for the presence of dimerized sensor. It was prepared by labeling SNAP_mCherry_HCA with a BG−BG molecule that induces a covalent dimerization of SNAP-tag fusion proteins (CoDis).[48]

Sulfonamide Derivatives Sensing. The labeled fusion proteins were diluted to a concentration of 250 nM into buffers (50 mM HEPES pH 7.2, 50 mM NaCl, 2% DMSO) adjusted to defined concentrations of benzenesulfonamide or ethoxzolamide, respectively. The samples were incubated for at least 2 h at room temperature before fluorescence measurements. Fluorescence emission spectra were recorded on an Infinite M1000 spectrofluorometer (TECAN) using black 96-well plates (FALCON). Both the excitation and emission bandwidth for all measurements was set to 10 nm. The spectra were measured with a step size of 1 nm. The excitation wavelength for SNAP_mCherry_HCA(PEG_{11}-Cy5-SA) and SNAP_mCherry_HCA(PEG_{11}-Cy5) was set to 530 nm. The emission spectra were recorded from 580 to 700 nm. The excitation (exc) and emission (em) wavelengths for SNAP_CLIP_HCA labeled with BG derivatives **1**−**6** and CT derivatives were as follows: (i) BG-PEG_{11}-Cy5-SA or BG-PEG_{11}-Cy5 (control) and CT-547, exc 500 nm, em 540−700 nm; (ii) BG-PEG_{11}-Cy5-SA or BG-PEG_{11}-Cy5 and CT-fluorescein, exc 485 nm, em 500−700 nm; (iii) BG-PEG_{11}-fluorescein-SA or BG-PEG_{11}-fluorescein and CT-547, exc 485 nm, em 500−700 nm; (iv) BG-PEG_{11}-fluorescein-SA or BG-PEG_{11}-fluorescein and CT-360, exc 360 nm, em 400−600 nm. To evaluate the experimental data, the ratio of the donor fluorophore

(46) Keppler, A.; Pick, H.; Arrivoli, C.; Vogel, H.; Johnsson, K. *Proc. Natl. Acad. Sci. U.S.A.* **2004**, *101*, 9955.
(47) Hunt, J. B.; Rhee, M. J.; Storm, C. B. *Anal. Biochem.* **1977**, *79*, 614.
(48) Lemercier, G.; Gendreizig, S.; Kindermann, M.; Johnsson, K. *Angew. Chem., Int. Ed. Engl.* **2007**, *46*, 4281.

emission intensity over the acceptor fluorophore emission intensity was plotted against the sulfonamide concentration. To obtain the binding constant for competing ligands $K_d^{comp,ligand}$, the data were fit to the following binding isotherm

$$r = r_{zero} + \frac{r_{sat} - r_{zero}}{1 + \frac{K_d^{comp,ligand}}{[ligand]}} \quad (1)$$

with r being the experimental emission ratio of donor vs acceptor, [ligand] the concentration of the corresponding sulfonamide derivative, and r_{zero} and r_{sat} the emission ratio in absence and presence of ligand, respectively. Fits were performed with Origin 7.5 (OriginLab Corporation) with free fit parameters $K_d^{comp,ligand}$, r_{zero}, and r_{sat}.

Effective Molarity. We estimated the effective molarity of the intramolecular ligand of SNAP_mCherry_HCA(PEG_{11}-Cy5-SA) by measuring binding of free BG-PEG_{11}-Cy5-SA to SNAP_mCherry_HCA in competition with free benzenesulfonamide. To do this we quenched SNAP_mCherry_HCA with BG, so it could no longer covalently react with BG-PEG_{11}-Cy5-SA. BG was added to a final concentration of 10 μM to a solution of 5 μM SNAP_mCherry-_HCA in 50 mM HEPES pH 7.2, 50 mM NaCl, 1 mM DTT. For the competition assays, solution of quenched SNAP_mCherry_HCA (250 nM) and different concentrations of free BG-PEG_{11}-Cy5-SA (1 μM, 10 μM, 20 μM) were titrated with benzenesulfonamide over a concentration range from 10 nM to 10 mM. Samples were incubated for at least 2 h at room temperature before fluorescence was measured with an EnVision Xcite multilabel reader (PerkinElmer, Inc.). The following filters were used for the FRET assays: excitation filter at 531 nm (bandwidth 25 nm) and emission filters at 595 nm (bandwidth 60 nm) and at 665 nm (bandwidth 7.5 nm). The $K_d^{comp,SA}$ values for displacement with benzenesulfonamide for each concentration of free BG-PEG_{11}-Cy5-SA were obtained from the titration curves by fitting to eq 1.

Activity Test of HCA. To test for the presence of Zn^{2+} in the active site of HCA in SNAP_mCherry_HCA, hydrolytic activity assays with the chromogenic substrate *p*-nitrophenyl acetate were performed. The assays were carried out using 1 μM SNAP_mCherry_HCA and 1 mM *p*-nitrophenyl acetate in 50 mM HEPES, pH 7.2, 50 mM NaCl, 10% acetonitrile. To confirm that the observed hydrolysis of *p*-nitrophenyl acetate is due to HCA activity, a control assay in the presence of the strong HCA inhibitor ethoxzolamide (1.2 μM) was carried out. The initial rates of the HCA catalyzed reactions were measured by following the hydrolysis of *p*-nitrophenyl acetate at 348 nm using a SPECTRAmax 340 spectrophotometer (Molecular Devices). The fraction of HCA containing Zn^{2+} in the active site was determined by comparing the measured rate to the initial rate of SNAP_mCherry_HCA saturated with $ZnCl_2$, which was defined as 100% activity.

Zn^{2+} Sensing. Labeled fusion proteins were used at a concentration of 250 nM and were dissolved into solutions of defined EGTA-Zn^{2+} buffers (50 mM HEPES pH 7.2, 50 mM NaCl) with controlled concentrations of free Zn^{2+} ions, formulated using the equation

$$K_d = \frac{[Zn^{2+}]_{free}[EGTA]_{total}}{[Zn^{2+}]_{total} - [Zn^{2+}]_{free}} - [Zn^{2+}]_{free} \quad (2)$$

where $[Zn^{2+}]_{free}$ is the concentration of free Zn^{2+}, $[EGTA]_{total}$ is the total concentration of ethylene glycol tetraacetic acid (EGTA), and $[Zn^{2+}]_{total}$ is the total concentration of Zn^{2+} and using a dissociation constant of EGTA for Zn^{2+} at pH 7.2 of $K_d = 2.8$ nM. This constant was obtained as described[49] based on a $K_d = 4.27$ nM at pH 7.11 and decreasing this value by 0.02 log units per 0.01 increase in pH. Detailed formulations of the free Zn^{2+} solutions are reported in the Supporting Information (Table S1). Samples were incubated for at least 2 h at room temperature before fluorescence measurements. Fluorescence emission spectra were recorded on an Infinite M1000 spectrofluorometer (TECAN) using black 96-well plates (FALCON). The excitation wavelength for SNAP_mCherry_*apo*HCA(PEG_{11}-Cy5-SA) and SNAP_mCherry_*apo*HCA(PEG_{11}-Cy5) was set to 530 nm, with excitation and emission bandwidths set to 10 nm. The emission spectra were recorded from 580 to 700 nm with a step size of 1 nm. The ratio of the fluorescence emission intensities of mCherry (610 nm) over Cy5 (670 nm) was plotted vs the free Zn^{2+} concentration. The data were fit to the binding isotherm (eq 1) in which r_{zero} is the emission ratio in absence of free Zn^{2+}, r_{sat} is the emission ratio at saturating concentrations of free Zn^{2+}, and [ligand] is the concentration of free Zn^{2+}. The obtained $K_d^{comp,ligand}$ is in these measurements an apparent K_d^{app} of SNAP_mCherry_HCA(PEG_{11}-Cy5-SA) for free Zn^{2+}.

Förster Distance and FRET Efficiencies. We determined the Förster distance for the pair mCherry and Cy5 by a standard approach.[40] The overlap integral $J(\lambda)$ expresses the degree of spectral overlap between the donor emission F_D and the acceptor absorption ε_A, which both depend on the wavelength λ. With the integrated fluorescence intensity F_D corresponding to the region of overlap normalized to 1, one obtains $J(\lambda)$ with the equation

$$J(\lambda) = \int_0^\infty F_D(\lambda)\, \varepsilon_A(\lambda)\lambda^4\, d\lambda \quad (3)$$

To calculate the Förster distance, we additionally require the orientation factor κ^2, the fluorescence quantum yield of the donor (Q_D), and the refractive index of the medium n, with Avogadro's number N_A according to eq 4.[50]

$$R_0^6 = \frac{9(\ln 10)\kappa^2 Q_D J(\lambda)}{128\pi^5 N_A n^4} \quad (4)$$

We computed the overlap integral of mCherry and Cy5 using publicly available spectra of the emission of mCherry[51] and the absorption of a protein-bound Cy5 analog (SNAP-tag labeled with BG-647),[52] and with $\varepsilon(Cy5)_{647nm} = 250\,000\ M^{-1}\ cm^{-1}$ we obtained a value of $J(\lambda) = 2.08 \times 10^{-12}\ M^{-1}\ cm^3$ (Supporting Information, Figure S2). Using standard values $\kappa^2 = 2/3$ (corresponding to randomized relative fluorophore orientations) and $n = 1.4$[40] and a fluorescence quantum yield of 0.22 for mCherry,[53] we obtained a Förster distance of $R_0 = 64.1$ Å with eq 4. We then computed R_0 with the measured spectra of SNAP_mCherry_HCA and SNAP-_CLIP_HCA labeled with BG-PEG_{11}-Cy5-SA and obtained a similar value with $R_0 = 63.3$ Å. To calculate effective distances based on FRET efficiencies, we used a rounded value of $R_0 = 63$ Å. For these experiments, quantitative SNAP-tag labeling was ensured by an excess of BG-PEG_{11}-Cy5-SA and long reaction times (cf. Biosensor Labeling). After reaction and purification, we checked the relative absorption of mCherry and Cy5. The absorption data were in accord with quantitative labeling using the extinction coefficients at the absorption maxima of $\varepsilon(mCherry)_{587nm} = 72\,000\ M^{-1}\ cm^{-1}$[53] and $\varepsilon(Cy5)_{647nm} = 250\,000\ M^{-1}\ cm^{-1}$ and correcting for the absorption of Cy5 at the absorption maximum of mCherry, which amounted to $\varepsilon(Cy5)_{587nm} = 0.236\varepsilon(Cy5)_{647nm}$. The latter value was determined by measuring the absorption spectrum of SNAP_

(49) Grynkiewicz, G.; Poenie, M.; Tsien, R. Y. *J. Biol. Chem.* **1985**, *260*, 3440.

(50) Braslavsky, S. E.; Fron, E.; Rodriguez, H. B.; Roman, E. S.; Scholes, G. D.; Schweitzer, G.; Valeur, B.; Wirz, J. *Photochem. Photobiol. Sci.* **2008**, *7*, 1444.

(51) Fluorophore excitation and emission spectra: http://www.tsienlab.ucsd.edu/Documents/REF%20-%20Fluorophore%20Spectra.xls (accessed Nov 24, 2008).

(52) SNAP-vitro 647: http://www.covalys.com/fileadmin/documents/bg647_ex_spectrum.rtf. (accessed Feb 19, 2009).

(53) Shaner, N. C.; Lin, M. Z.; McKeown, M. R.; Steinbach, P. A.; Hazelwood, K. L.; Davidson, M. W.; Tsien, R. Y. *Nat. Methods* **2008**, *5*, 545.

CLIP_HCA labeled with BG-PEG_{11}-Cy5-SA. To ensure equal protein concentrations in the measurements of F_{DA} and F_D, they were adjusted relative to mCherry absorption, using the extinction coefficients and determined correction factor for Cy5 absorption at 587 nm.

Acknowledgment. This work was supported by the Swiss National Science Foundation and the Human Frontier Science Program. E.N. was supported by the JSPS Research Fellowships for Research Abroad. M.J.H. was supported by a postdoctoral grant (Hi 1363/1-1) from the Deutsche Forschungsgemeinschaft (DFG). We thank Christopher Chidley, Dr. Arnaud Gautier, and Dr. Armin Lambacher for valuable discussions. We thank Dr. Simone Schmitt for technical assistance with the SE-FPLC measurements.

Supporting Information Available: Synthetic procedures and characterizations of fusion proteins. This material is available free of charge via the Internet at http://pubs.acs.org.

JA900149E